Inorganica Chimica Acta 447 (2016) 127–133

Contents lists available at ScienceDirect

Inorganica Chimica Acta

journal homepage: www.elsevier.com/locate/ica

Synthesis, physicochemical and biological studies of a ternary Co(II) complex with sulfaquinoxaline and 2,2′-bipyrimidine as ligands

C. Villa-Pérez [a], J.F. Cadavid-Vargas [a], G.E. Camí [b], F. Giannini [b], M.E. Chacón Villalba [a], G. Echeverria [c], I.C. Ortega [d], G.C. Valencia-Uribe [d], S.B. Etcheverry [a], D.B. Soria [a,*]

[a] CEQUINOR, Departamento de Química, Facultad de Ciencias Exactas, Universidad Nacional de la Plata, 47 y 115, 1900 La Plata, Argentina
[b] Área de Química General e Inorgánica, Departamento de Química, Facultad de Química, Bioquímica y Farmacia, Universidad Nacional de San Luis, Chacabuco y Pedernera, 5700 San Luis, Argentina
[c] IFLP-LANADI, Departamento de Física, Facultad de Ciencias Exactas, Universidad Nacional de La Plata, 1900 La Plata, Argentina
[d] GIAFOT, Departamento de Química, Facultad de Ciencias, Universidad Nacional de Colombia-Sede Medellín, Calle 59 A Nº. 63-020, Medellín, Colombia

ARTICLE INFO

Article history:
Received 13 December 2015
Received in revised form 17 February 2016
Accepted 30 March 2016
Available online 6 April 2016

Keywords:
Sulfaquinoxaline
2,2′-Bipyrimidine
Co(II) complex
Spectroscopic properties
X-ray structure
Biological properties

ABSTRACT

A novel ternary complex of Cobalt(II) with 4-amino-*N*-2-quinoxalinylbenzenesulfonamide (sulfaquinoxaline, SQO), and 2,2′-bipyrimidine (Bpym) as ligands has been prepared. The complex has been characterized based on elemental analyses, FTIR and Raman spectroscopy. Its structure, $[Co(SQO)_2(Bpym)]$ was determined by X-ray diffraction methods. It crystallizes in the triclinic $P\bar{1}$ space group with $a = 10.5381(2)$, $b = 13.6469(2)$, $c = 13.8409(3)$ Å, $\alpha = 95.058(2)°$, $\beta = 93.769(2)°$, $\gamma = 93.750(2)°$ and $Z = 2$ molecules per unit cell. Thermogravimetric (TG) and differential thermal analysis (DT) were also studied.

The aquatic toxicity of the complex was evaluated on the two following test organisms: *Danio rerio* (cebritas) y *Cyprinus carpio haematopterus* (carpas koi). Antibacterial activity was screened against *Escherichia coli* (ATCC 8739), *Salmonella typhimurium* (ATCC 14028), *Staphylococcus aureus* (ATCC 49775) and *Bacillus cereus* (ATCC 10987). The antiproliferative effect of the tested complex $[Co(SQO)_2(Bpym)]$ in the human osteoblast (MG-63) cell line was also studied.

1. Introduction

Sulfonamides are the oldest chemotherapeutic agents used for antibacterial therapy. It is well known that they play an important role in veterinary mass treatments [1,2]. In the last twenty years there has been growing interest to reduce the environmental load of veterinary pharmaceuticals from intensively reared animals [3,4]. Sulfaquinoxaline (SQO) is a drug routinely used in veterinary prophylactic mass treatment to prevent coccidiosis and bacterial infections. One of the reasons is its low cost and broad-spectrum activity (antibacterial and anticoccidial) suitable for routine mass treatment (prophylactic/metaphylactic). The use of metal-based therapeutics for both diagnosis and treatment of diseases constitutes a new field of increasing interest. Metal ions have always been relevant in biological systems, [5] with several diverse features that establish the characteristics of metal coordination systems, based on the spatial arrangement of the ligands around the metal ion.

In view of the versatile importance of metal complexes, and in order to identify their coordination properties, we have previously reported the results of the structural and electronic investigations of p-cyanobenzenosulfonamide, and its copper(II) complex [6]. We also prepared and characterized a new copper(II) complex, $[Cu(ClNbsa)_2(NH_3)_2]$ with 4-chloro-2-nitrobenzenesulfonamide as ligand [7]. Recently we have published the results for two new complexes of Ni(II) and Zn(II) with the same ligand [8]. Due to the interesting coordination chemistry and biological properties of the sulfonamide complexes, we here describe the synthesis of a ternary complex of Co(II) with SQO and 2,2′-bipyrimidine as ligands to further expand the research to include other complexes. Its characterization by means of X-ray diffraction, thermogravimetry, FTIR and Raman spectra is also discussed. It should be noted that the crystallographic structure of ternary sulfaquinoxaline coordination compounds has not yet been published. In fact, only one Cd(II) binary complex structure was reported in the literature at the date of this publication [9]. To investigate the potential use of the new complex in biological systems, different models (bacteria, osteoblast-like cells and fish) were used. The aquatic and cell toxicity as well as antibacterial activity have been studied. Although ternary cobalt complexes with sulfaquinoxaline have

* Corresponding author.
E-mail address: soria@quimica.unlp.edu.ar (D.B. Soria).

http://dx.doi.org/10.1016/j.ica.2016.03.043
0020-1693/

not been previously reported, a few examples with sulfadiazine (4-amino-*N*-(pyrimidin-2-yl)benzenesulfonamide), and dimethylformamide, methanol or pyridine as coligand have been reported [10–12].

2. Experimental

2.1. Physicochemical studies

2.1.1. Materials and methods

The FTIR spectra were carried out with a Bruker EQUINOX 55 spectrophotometer (Billerica, MA, USA), in the range from 4000 to 400 cm^{-1} using the KBr pellet technique, with a spectral resolution of 4 cm^{-1}. The Raman spectra were recorded with a Bruker IFS 66 FTIR spectrophotometer (Billerica, MA, USA), provided with the NIR Raman attachment, with a resolution of 4 cm^{-1}. The electronic absorption spectra of the compounds were measured in two different conditions: in freshly prepared DMSO (Sigma Chemical Co., St. Louis, MO, USA) solutions in the 200–800 nm spectral range, and in solid state with KBr reference pellet. They were recorded with a Hewlett–Packard 8452-A diode array spectrophotometer (Agilent Technologies Ltd., Santa Clara, CA, USA), using 10 mm quartz cells. DT and TG analyses were performed using Shimadzu TGA-50 and DTA-50H units (Kyoto, Japan), at a heating rate of 5 °C min^{-1} and oxygen flow of 50 ml min^{-1}.

2.1.2. Synthesis of the complex

All the reagents were obtained from Sigma Chemical Company (St. Louis, MO, USA) and used without further purification. The Cobalt(II) complex was prepared by direct reaction of ethanol solutions of sodium sulfaquinoxaline, 2,2′-bipyrimidine and $CoCl_2{\cdot}6H_2O$ in the 1:1:1 M ratio under continuous stirring. The resulting solution was stirred during ca. 6 h at room temperature and was then left to stand. Slow evaporation of the solution provided well-developed orange crystals that were suitable for X-ray diffraction. They were collected by filtration, washed, dried and subjected to elemental microanalyses. The elemental analysis (%) for $C_{36}H_{32}CoN_{12}O_6S_2$ gave the following results: calc.: C, 50.76; H, 3.79; N, 19.73; S, 7.53; Found: C, 53.05; H, 3.75; N, 21.09; S, 7.76%. The yield was 78.7%. The stability of the complex was studied spectrophotometrically in aqueous solution at room temperature. No spectral changes were observed during a period of 24 h (see Fig. S1 in the Supplementary information).

2.1.3. X-ray diffraction data

The measurements were performed on an Agilent Gemini Diffractometer with an EOS CCD detector equipped with a graphite-monochromated Cu Kα ($\lambda = 0.71073$ Å) radiation. X-ray diffraction intensities were collected (ω scans with θ and κ-offsets), integrated and scaled with CrysAlisPro (Agilent Technologies Ltd., Yarnton, Oxfordshire, UK) [13] suite of programs. The unit cell parameters were obtained by least-squares refinement (based on the angular settings for all collected reflections with intensities larger than seven times the standard deviation of measurement errors) using CrysAlisPro. Data were corrected empirically for absorption employing the multi-scan method implemented in CrysAlisPro. The structure was solved by direct methods with SHELXS-97 (Göttingen, Lower Saxony, Germany) [14] and the molecular model refined by full-matrix least-squares procedure on F^2 with SHELXL-97 [15,16]. Two water oxygen positions were determined from a difference Fourier map phased with the refined positions and isotropic thermal parameters of all atoms of the X-ray model, not belonging to water molecules. After refinements, including the two water molecules, the calculated residual electron density map showed three additional peaks of the electron densities greater than 1 e $Å^{-3}$ which was associated with crystallizing disordered water and could not be modeled adequately in terms of atomic contributions. Hence, the quality of refinement of the least-squares fitting was limited (agreement R_1 factor equal to 0.089). Therefore, we proceeded with the refinement of Co(II) complex resorting to a described procedure [17], implemented in the program SQUEEZE included in the PLATON [18] suite of programs. As a result, the overall quality of the refinement improved and the R_1 value dropped to 0.070. The atomic positions of the water hydrogen atoms were calculated by combined geometric and force-field calculation on the basis of hydrogen-bonding interactions using the computer program HYDROGEN [19] implemented in the WINGX system [20]. The hydrogen atoms of the amino groups were positioned from the difference Fourier density map while the rest of the hydrogen atoms were positioned stereo-chemically. Further refinements were performed with the hydrogen positions riding on the corresponding bound atom. Crystal data, data collection and structure refinement details are summarized in Table 1. Crystallographic structural data have been deposited at the Cambridge Crystallographic Data Centre (CCDC). Any request to the CCDC for this material should quote the full literature citation and the reference number CCDC 1402537.

2.2. Biological studies

2.2.1. Aquatic toxicity

The toxic effect of the complex was evaluated using a toxicity test on fish. The static technique recommended by the U.S. Fish and wildlife Service, Columbia National Fisheries Research Laboratory [21] was modified in order to use lower amounts of the tested compounds [22]. Fish of the species *Danio rerio* and *Cyprinus carpio haematopterus* were hatched and raised in our laboratory until they were 90 days old. The first one reached an average length of 1–2 cm and 100 mg of weight, while the second one grew in average

Table 1
Crystal data and structure refinement for $[Co(SQO)_2Bpym]{\cdot}2H_2O$.

Empirical formula	$C_{36}H_{32}CoN_{12}O_6S_2$
Formula weight	851.79
T (K)	297(2) K
λ (Å)	0.71073
Crystal system	triclinic
Space group	$P\bar{1}$
Unit cell dimensions	
a (Å)	10.5381(2)
b (Å)	13.6469(2)
c (Å)	13.8409(3)
α (°)	95.058(2)
β (°)	93.769(2)
γ (°)	93.750(2)
V ($Å^3$)	1973.37(6)
Z	2
D_{calc} (g cm^{-3})	1.434
Absorption coefficient (mm^{-1})	0.602
$F(000)$	878
Crystal size (mm^3)	0.308 × 0.200 × 0.095
θ-range for data collection (°)	3.00–26.50
Index ranges	$-13 \leqslant h \leqslant 13$, $-16 \leqslant k \leqslant 17$, $-17 \leqslant l \leqslant 17$
Reflections collected/unique [R_{int}]	24088/8066 [0.0327]
Completeness to $\theta = 26.50°$	98.5%
Absorption correction	semi-empirical from equivalents
Maximum and minimum transmission	1.00000 and 0.97248
Refinement method	full-matrix least-squares on F^2
Data/restraints/parameters	8066/4/514
Goodness-of-fit (GOF) on F^2	1.047
Final R indices [$I > \sigma(I)$]	$R_1 = 0.0438$, $wR_2 = 0.1058$
R indices (all data)	$R_1 = 0.0658$, $wR_2 = 0.1160$
Largest diff. peak/hole (e $Å^{-3}$)	0.366/−0.374

until 3–4 cm with 1 g of weight. Four lots with ten fish each were exposed to each potentially toxic agent in a 2 L vessel. The percent mortality was checked at 96 h and after that time, mobility and morphological aspects were studied during a period of seven additional days. Stock solutions (20 mg ml^{-1}) were prepared using DMSO (20%) as solvent and sonified for 1 h. After the total dissolution of the compounds, the appropriate amount of the stock solution was added to each 2 L vessel to obtain a final concentration of 60 μg ml^{-1} (with DMSO concentration under 0.1%). A batch with water as negative toxicity control and another one containing water with DMSO (0.1%) as potential toxicity were used. This assay has been previously reported for synthetic and natural compounds [23].

2.2.2. Antibacterial activity

The antibacterial activity was tested against both Gram-negative and Gram-positive bacteria using the agar diffusion method. Four strains of bacteria derived from the American Type Culture Collections (ATCC), namely, *Escherichia coli* (ATCC 8739), *Salmonella typhimurium* (ATCC 14028), *Staphylococcus aureus* (ATCC 49775) and *Bacillus cereus* (ATCC 10987) were used.

The cultivation and assay medium for all the strains were Nutrient agar and Mueller Hinton agar, respectively. The Kirby and Bauer agar diffusion method was applied [24]. A McFarland 0.5 standard suspension was prepared for each microorganism and was seeded on the assay agar (~1.5×10^8 bacteria per milliliter) [25,26]. Stock solutions (50 mg ml^{-1}) of the compounds (6% DMSO) were prepared and sterilized by filtration using 0.45 μm millipore filters (Acrodisc nylon membrane). After the seeding of the bacteria, MN 827 ATD disks (6 mm in diameter) were impregnated with doses of the compounds from 50 to 400 μg. A disk with 6% DMSO solution was used as control. In order to accomplish a better diffusion of the compound, the inoculated agar was kept at 4 °C for 3 h and then the plates were incubated at 37 °C during a period of 24 h. All the assays were carried out three times.

2.2.3. Cytotoxicity screening

The human osteosarcoma MG-63 cell line was purchased from ATCC (CRL1427™). Cells were grown in Dubelcco's Modified Eagle Medium (DMEM) (Gibco, Gaithersburg, MD, USA), containing 10% fetal bovine serum (Internegocios S.A., Argentina), 100 U ml^{-1} penicillin and 100 μg ml^{-1} streptomycin at 37 °C in a 5% CO_2 atmosphere. Cells were seeded in a 75 cm^2 flask (Corning, Princeton, NJ, USA), and when 70–80% confluence was reached, they were subcultured (1 ml TrypLE™ Gibco, Gaithersburg, MD, USA, *per* 25 cm^2 flask). For experiments, cells were grown in multi-well plates. When cells reached the desired confluence, the monolayers were washed with DMEM and incubated under the conditions described below.

2.3. MTT (methyl tetrazolium) assay

The 3-(4,5-dimethylthiazol-2-yl)-2,5-diphenyltetrazolium bromide (MTT) (Sigma Chemical Co., St. Louis, MO, USA) assay was performed according to Mosmann [27]. Briefly, cells were seeded in a 96-well plate, allowed to attach for 24 h, and treated with different concentrations of the complex, ligands and cobalt chloride at 37 °C for 24 h. Afterward, the medium was changed and the cells were incubated with 0.5 mg ml^{-1} of MTT under normal culture conditions for 3 h. Cell viability was marked by the conversion of the tetrazolium salt MTT to a colored formazan by mitochondrial dehydrogenases. Color development was measured spectrophotometrically with a microplate reader (model 7530, Cambridge Technology, USA) at 570 nm after cell lysis with DMSO (Sigma Chemical Co., St. Louis, MO, USA) (100 μL per well). Cell viability was plotted as the percentage of the control value.

For the antibacterial activity and MTT assays, statistical analysis of the data was carried out by ANOVA, followed by the Tukey's range test to discriminate if there is statistical difference among the means. The statistical analysis was performed using the software STATGRAPHICS Centurion XVI.I.

3. Results and discussion

3.1. Crystal structure

The complex consists of one neutral [$Co(SQO)_2$Bpym] unit and two water molecules. It crystallizes in the centrosymmetric triclinic $P\bar{1}$ space group with $Z = 2$ molecules per unit cell. Fig. 1 shows an ellipsoid plot of the Co(II) coordination sphere together with the used numbering scheme. Relevant bond distances and angles around the metal center are reported in Table 2. Two inequivalent SQO and one Bpym ligands are coordinated to the Co(II) in a bidentate chelating mode. A similar coordination mode for the SQO ligand has been found in another complex [9]. The Co(II) ion exhibits a CoN_6 coordination sphere. Calculation of the degree of distortion of the CoN_6 coordination polyhedron with respect to several ideal six-vertex polyhedra, with the help of the SHAPE software by using the continuous shape measure theory [28], indicates that the coordination sphere can be considered between the octahedron (OC-6) and the trigonal prism (TPR-6) geometries. Values of 4.543 and 12.003 were calculated for the OC-6 and the TPR-6 polyhedra, respectively. The geometry of the complex found by X-ray seems to be closer to the octahedral OC-6 geometry (see Table S1).

The two Co–N (Bpym) bond distances are slightly shorter than those of the SQO ligand (see Table 2), but similar to those values, reported in the literature for other Co complexes with Bpym ligand [29]. The sulfaquinoxaline intramolecular parameter values (not

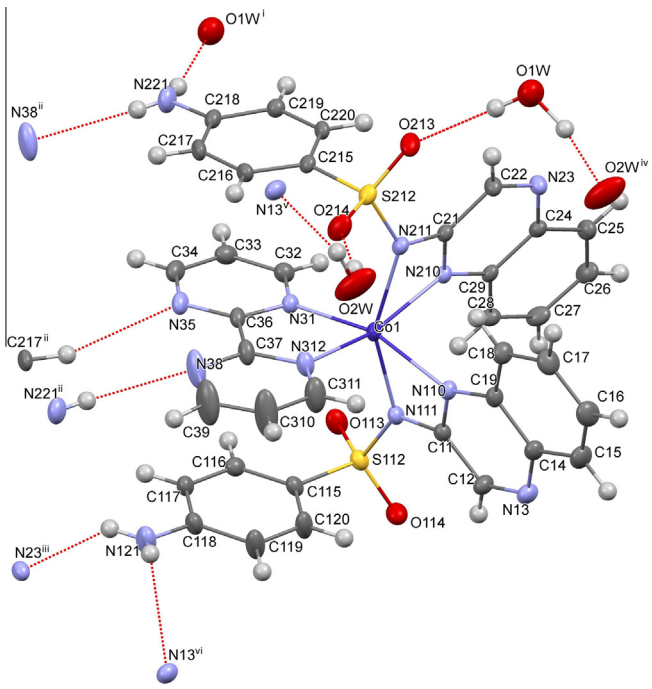

Fig. 1. Plot of [$Co(SQO)_2$Bpym]·$2H_2O$ complex showing the labeling of the independent non-H atoms and their displacement ellipsoids at the 20% probability level. Dashed lines denote the H-bonding structure. Intermolecular H-bond interactions are also shown. Symmetry transformations used to generate equivalent atoms: (i) $-x+2, -y+1, -z+1$; (ii) $-x+2, -y+1, -z$; (iii) $x, y, z-1$; (iv) $-x+2, -y+2, -z+1$; (v) $x+1, y, z$; (vi) $-x+1, -y+2, -z$.

Table 2
Bond lengths (Å) and angles (°) around the metal center for $[Co(SQO)_2Bpym]\cdot 2H_2O$.

Co1–N31	2.100(2)	N312–Co1–N110	95.69(8)
Co1–N312	2.106(2)	N31–Co1–N211	99.94(8)
Co1–N111	2.132(2)	N312–Co1–N211	100.27(9)
Co1–N211	2.153(2)	N111–Co1–N211	151.85(8)
Co1–N110	2.166(2)	N211–Co1–N210	62.08(7)
Co1–N210	2.171(2)	N211–Co1–N110	98.32(7)
		N31–Co1–N111	102.08(7)
N31–Co1–N312	77.32(8)	N312–Co1–N111	101.51(9)
N31–Co1–N210	103.31(7)	N111–Co1–N110	61.96(7)
N110–Co1–N210	88.63(7)	N111–Co1–N210	95.68(7)
N111–Co1–N211	151.85(8)	N110–Co1–N31	161.34(7)
N210–Co1–N312	162.31(8)		

Table 3
Hydrogen bonds for $[Co(SQO)_2Bpym]\cdot 2H_2O$ (Å and °).[a]

	D–H	H···A	D···A	D–H···A
N221–H222···O1w^{i}	0.87	2.23	3.106(4)	175.2
N221–H221···N38^{ii}	0.83	2.42	3.174(3)	151.6
N121–H122···N23^{iii}	0.87	2.43	3.129(3)	138.8
O1w–H12w···O2w^{iv}	0.84	1.91	2.747(4)	177.6
O1w–H11w···O213	0.88	2.05	2.931(3)	178.4
O2w–H21w···O214	0.85	1.99	2.812(3)	164.6
O2w–H22w···N13^{v}	0.87	2.15	3.024(4)	173.9
N121–H121···N13^{vi}	0.86	2.56	3.346(3)	153.9

[a] For symmetry operations see Fig. 1.

listed in Table 2) are similar to those that we previously reported for other sulfonamide complexes [6–8]. The bite angles of the SQO and Bpym ligands, are the smallest bond angles around the metal center found in the literature (see Table 2) [30,31]. These small angles may be part of the cause of the polyhedron distortion. In the two inequivalent SQO ligands, the angles between the sulfonamide ring and the quinoxaline group are 81.1° and 75.2°. When considering the stacking effect, the aniline moieties of all SQO ligands are approximately arranged in a parallel way to the Bpym ligand. The distances, calculated from benzene centroids to the Bpym mean atomic plane, are 3.538 and 3.479 Å. Also, along the *b* axis, the quinoxaline groups are disposed giving rise to intra and intermolecular π···π stacking interactions which could enhance the stability of the complex [32,33] (see Fig. 2). In addition, the 3D crystal structure is further stabilized by a network of hydrogen bonds linking sulfonamide and quinoxaline groups with Bpym ligand and hydration water molecules (see Table 3).

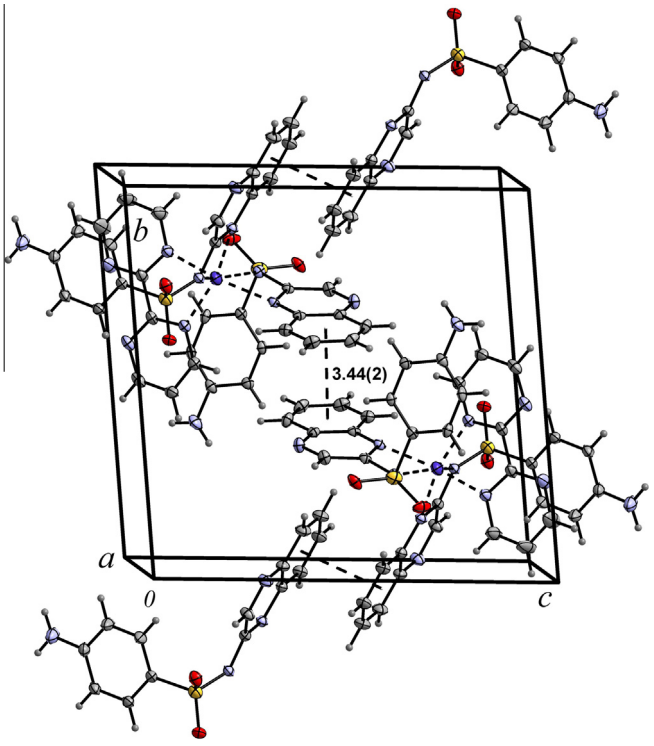

Fig. 2. Packing of the $[Co(SQO)_2Bpym]\cdot 2H_2O$ complex. In dashed lines are shown the intermolecular π···π stacking interactions along the *b* axis.

3.2. Spectroscopic properties

3.2.1. FTIR and Raman spectra

The observed FTIR and Raman bands for the complex are shown in Fig. 3. In the *ν*(OH) region, 3400–3880 cm^{-1}, the spectrum of the complex, shows the bands assignable to OH vibration of the uncoordinated two water molecules. The N–H vibrations of the NH_2 group 3343 and 3232 cm^{-1} are significantly shifted with respect to those of the free ligand (3359 and 3195 cm^{-1}) as a consequence of the hydrogen bonding interaction. These two bands also increase their intensities. The mixed nature of the two ligands produces many bands due to the C=C and C=N modes. The bands associated with these modes are observed in the 1600–1400 cm^{-1} range and they were shifted to the lower wavenumber upon complexation. The spectrum also shows a red shift in the sharp band at 1596 cm^{-1} attributed to the bending mode of the NH_2 group in comparison with the free ligand (1600 cm^{-1}). The 2,2′-bipyrimidine ligand can act as a terminal chelating or bis (chelating) ligand toward transition metal ions. IR spectroscopy is a useful tool for identifying the coordination mode [34,35]. The terminal chelating mode of Bpym is typically characterized by two peaks of nearly equal intensities at approximately 1580 and 1560 cm^{-1} (ring stretching modes of Bpym). However the presence of the bis-chelating coordination mode, is indicated either by an asymmetric doublet or a single strong broad band. The infrared spectrum of the complex shows a quasi-symmetric doublet at 1576 and 1556 cm^{-1} that points to the terminal coordination of Bpym in good

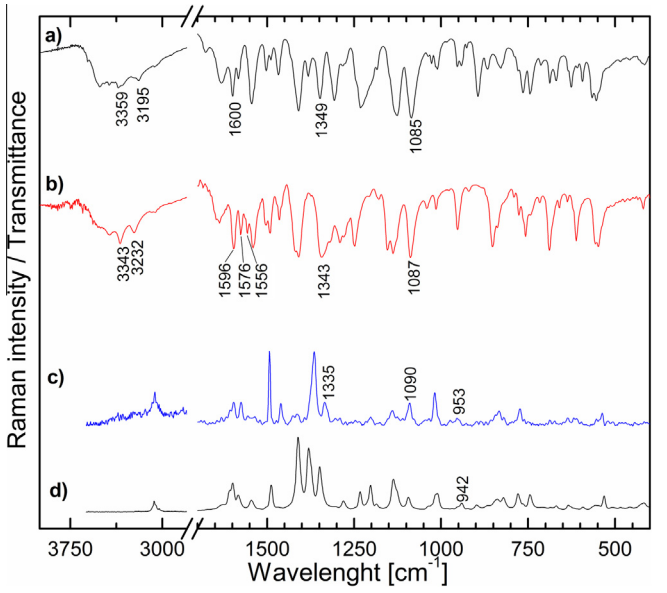

Fig. 3. (a) FTIR and (d) Raman spectra of the SQO ligand, (b) FTIR and (c) Raman spectra of the complex.

agreement with the X-ray result. The other relevant bands are those associated with the SO_2 group. The antisymmetric vibrational modes of the S=O bond in the complex are observed at 1343 and at 1349 cm^{-1} in the free ligand. In the Raman spectrum, this mode is observed as a weak band at 1335 cm^{-1}. Almost there is no change in the symmetric vibration modes, 1087 cm^{-1} in the complex and 1085 cm^{-1} in the free ligand. This band is observed at 1090 cm^{-1} in the Raman spectrum. The band associated to the S–N bond is observed at 942 cm^{-1} in the free ligand, which is shifted to 953 cm^{-1} in the complex. This fact is probably due to the shortening of the S–N bond length relative to that of the uncoordinated ligand [6–8].

3.3. Thermogravimetric study of the complex, TG–DT

The TG curve of the complex indicates (see Fig. S2) that the decomposition takes place in three steps. The first one corresponds to a weight loss of 4.70% which is consistent with the evolution of the two H_2O water molecules (loss of weight calculated 4.24%). This process takes place with two endothermic peaks observed in the DT curve at 54 °C and 60 °C. The second weight loss of 33.44% with an exothermic peak at 320 °C probably corresponds to the removal of the bipyrimidine ligand and one of the quinoxaline moieties (expected 33.68%). The third step corresponds to a weight loss of 42.12% consistent with the evolution of the remaining aniline moiety and of the sulfaquinoxaline ligands (calculated 44.10%). This process takes place with a sharp exothermic peak observed in the DT curve at 523 °C. Finally, the complete decomposition of the ligands occurs with the remaining SO_2 group with Co and a partial oxidation to cobalt sulfate, which has been characterized by infrared spectroscopy.

3.4. Aquatic toxicity

Percent mortality was checked at 24, 48, 72 and 96 h. No mortality, toxicity or lethal effects were observed during that period for the tested fish species at the used dose of the compounds. Mobility and other morphologic aspects (fins appearance and microscopic aspects) of the specimens were also evaluated, after the initial 96 h, during a period of seven days. No appreciable changes in fish activity, such as mobility or the appearance of the fins were observed.

3.5. Antibacterial assays

Taking into account the biological properties of SQO [36,37], the antibactericidal capacity of the Co(II) complex, the free ligands and the $CoCl_2{\cdot}6H_2O$ salt were tested. The results of each antibacterial assay are shown in Fig. 4.

For all the strains, neither the negative control (DMSO 6%) nor the Bpym ligand showed growth inhibition activity. The inhibition of the Gram-positive bacteria (*B. cereus* and *S. aureus*) was higher than that of the Gram-negative (*E. coli* and *S. typhimurium*) for all the tested doses ($p < 0.001$) (see Fig. 5). The complex caused wider

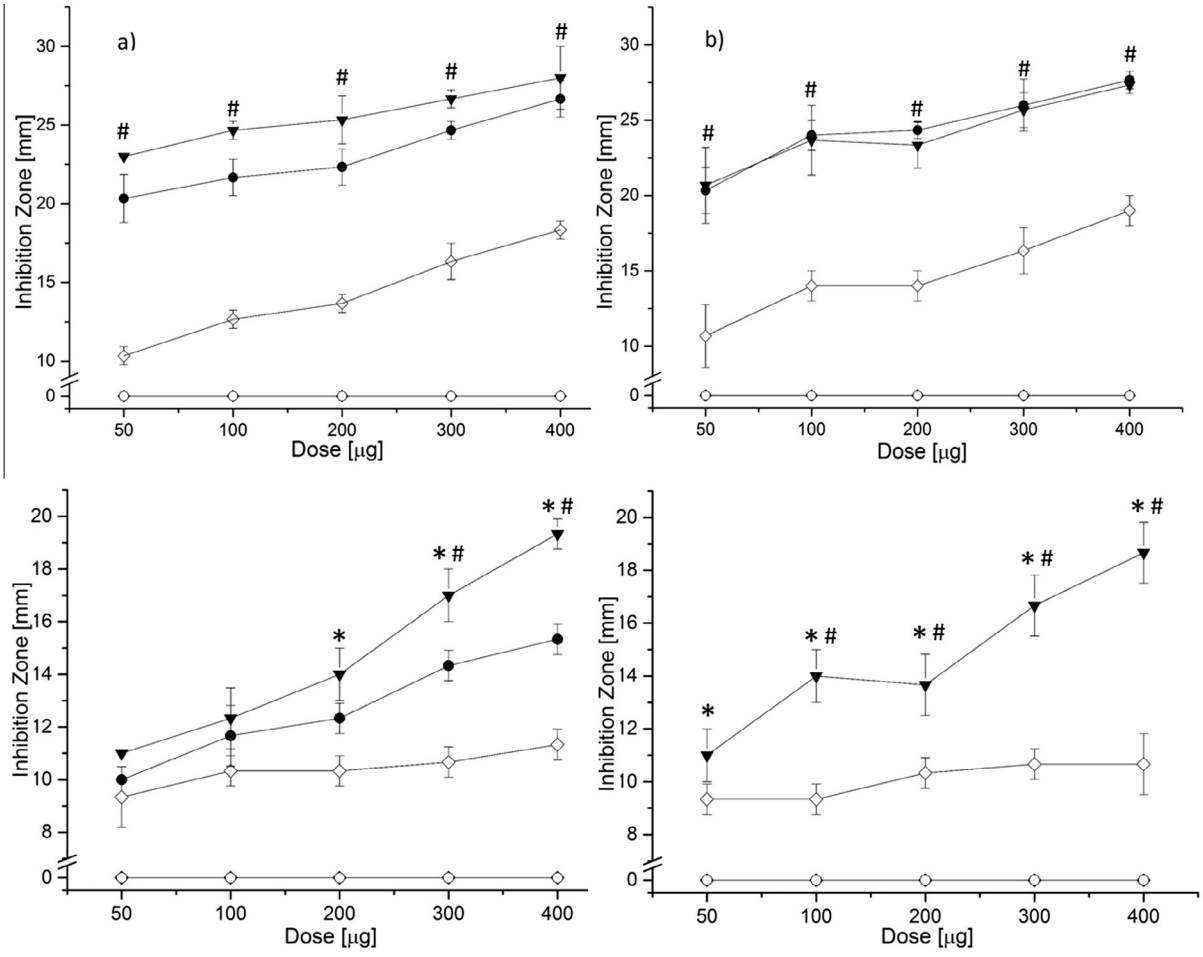

Fig. 4. Diameter of the inhibition zones ± SD [mm] for *B. cereus* (a), *S. aureus* (b), *E. coli* (c) and *S. typhimurium* (d) for the complex (▼), the free NaSQO (●) and the Co(II) salt (○). *Significant differences *versus* the free SQO ligand, $p < 0.001$. #Significant differences *versus* the $CoCl_2{\cdot}6H_2O$ salt, $p < 0.02$.

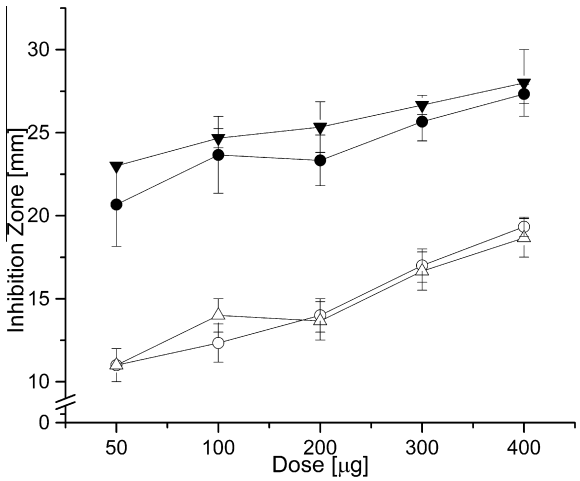

Fig. 5. Diameter of the inhibition zones ± SD [mm] for Gram positive (*B. cereus* (▼) and *S. aureus* (●)) and Gram negative bacteria (*E. coli* (○) and *S. typhimurium* (△)) for the complex.

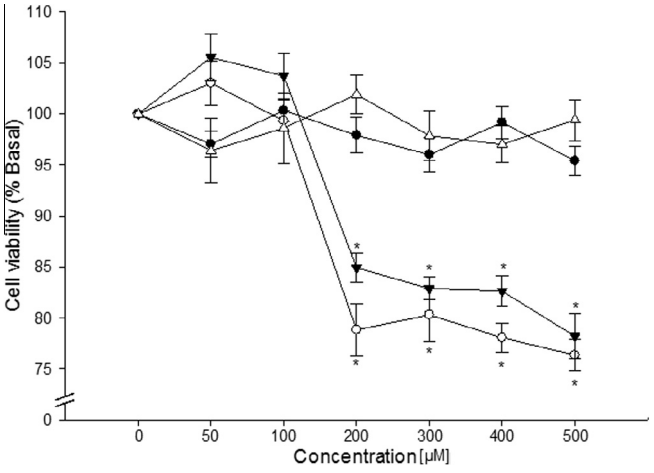

Fig. 6. MTT assay. Effect of [$Co(SQO)_2Bpym$] (▼)], NaSQO (●), Bpym and $CoCl_2$ (○) on osteoblast-like MG-63 cell proliferation. Cells were incubated at 37 °C for 24 h in serum-free DMEM without (0 µM represents basal condition) or with different concentrations of the compounds. Results are expressed as % basal and represent the mean ± SEM ($n = 10$). *Significant differences *versus* control, $p < 0.002$.

inhibition halos on *B. cereus* and *S. aureus* than the Co(II) salt in the whole dose range ($p < 0.001$). However there was not a significant difference between the complex and the free ligand (see Fig. 4a and b).

On the other hand, the complex caused higher growth inhibition than the metallic salt from 100 µg ($p < 0.001$) and 300 µg ($p < 0.02$), for the *S. typhimurium* and *E. coli* strains, respectively. In the same way a better performance of the complex compared with the SQO ligand was observed over the entire tested range for *S. typhimurium* ($p < 0.001$). While for *E. coli* the significant effect only can be observed for doses greater than 200 µg ($p < 0.001$) (Fig. 4c and d).

The behavior exhibited by the studied bacterial systems can likely be explained taking into account that in the ligands, the delocalization of pi-electrons is increased by the chelating effect. This fact enhances the liposolubility of the complex improving its permeation through the cell membrane and so the metabolic processes of the microorganisms are disturbed [38]. The bacterial death mechanism is probably associated with the inhibition of the dihydropteroate synthase enzyme, caused by the sulfonamide group [36], preventing in this way the synthesis of folic acid in the bacteria.

3.6. Cytotoxicity evaluation

MG-63 osteoblast cell line, is a cellular line originally isolated from a human sarcoma. MG-63 are relatively immature osteoblasts broadly used for testing biomaterials. These cells show several similarities with isolated human bone-derived cells. They were used in this work as a model of mammalian bone related cells [39,40]. The cytotoxic effect of the complex was evaluated against MG-63 cell line taking into account that Co (II) ions have shown cytotoxic effect against that cellular line [40].

The MTT test is a useful tool extensively used to investigate the antiproliferative actions of different compounds. MTT is a probe for metabolically active mitochondria. In these organelles MTT is reduced by the dehydrogenases to a colored compound which is extracted and determined spectrophotometrically [41]. If the mitochondrial metabolism is altered by a cytotoxic drug, the absorbance is reduced as it was observed for the complex and cobalt chloride in the range from 200 to 500 µM (see Fig. 6).

Fig. 6 shows the effect of increasing concentrations of the ligands (SQO and Bpym), cobalt chloride and the ternary complex in the range of 50–500 µM on cell viability on MG-63 cells. As can be seen from the figure, the free ligands did not exert any considerable cytotoxic effects over the whole range of concentrations, since no significant difference could be observed relative to the control. On the contrary, at 200 µM the ternary complex and cobalt chloride caused a decrease in the cell viability compared to control values ($p < 0.002$) and this effect was also observed up to 500 µM. In the range of the lower concentrations of the complex and the ion, no deleterious effects were measured.

The observed results show that the free ligands are not toxic for the MG-63 cell line while the complex and the free ion cause a moderate decrease in cell viability.

4. Conclusions

This study reports the synthesis and characterization of a ternary complex with sulfaquinoxaline and 2,2′-bipyrimidine as ligands. This new complex was structurally characterized for the first time via X-ray crystallography. It should also be noted that this is only the second time in which sulfaquinoxaline's crystal structure has been reported on, based on our review of the literature. Spectroscopic results (FTIR and Raman), are in a good agreement with the X-ray crystallographic data. Very scarce data are available regarding the aquatic toxicity of SQO and none for the complex, so evaluating the aquatic toxicity of the complex on different test organisms has been important. No mortality or lethal effects were observed. The prepared metal complex exhibited higher antimicrobial activities against *E. coli* and *S. typhimurium* than the parent ligand. The cytotoxicity study in osteoblast-like cells has shown no toxicity for the ligands and a weak deleterious action by the free ion and the complex.

In conclusion, these studies provide useful information about the physicochemical and biological properties of a new cobalt complex. The results show that it is a good drug for antibacterial treatment and do not produce important toxicity effect in vitro and in vivo models.

Acknowledgements

This work was partly supported by UNLP (11X/606 and 11X/690), CONICET (PIP 356, 1125 and 1529) and ANPCyT (PME06 2804, PICT06 2315 and PICT 2218-2008) from Argentina.

G.E., S.B.E. and D.B.S. are members of the Carrera del Investigador, CONICET, Argentina. C.V.P. and J.F.C.V. are fellowships from CONICET, Argentina. M.E.Ch.V. is member of Professional Staff of Comisión de InvestigacionesCientíficas, Provincia de Buenos Aires, Argentina (CICPBA).

Appendix A. Supplementary material

CCDC 1402537 contains the supplementary crystallographic data for this paper. These data can be obtained free of charge from The Cambridge Crystallographic Data Centre via www.ccdc.cam.ac.uk/data_request/cif. Supplementary data associated with this article can be found, in the online version, at http://dx.doi.org/10.1016/j.ica.2016.03.043.

References

[1] A.B.A. Boxall, D.W. Kolpin, B. Halling-Sørensen, J. Tolls, Environ. Sci. Technol. 37 (2003) 286A, http://dx.doi.org/10.1021/es032519b.
[2] P. Sukul, M. Spiteller, Rev. Environ. Contam. Toxicol. 187 (2006) 67, http://dx.doi.org/10.1007/0-387-32885-8_2.
[3] B. Halling-Sorensen, S.N. Nielsen, P.F. Lanzky, F. Ingerslev, H.C. Holten Lützhoft, S.E. Jorgensen, Chemosphere 36 (1998) 357, http://dx.doi.org/10.1016/S0045-6535(97)00354-8.
[4] M.H. Montforts, D.F. Kalf, P.L. van Vlaardingen, J.B. Linders, Sci. Total Environ. 225 (1999) 119, http://dx.doi.org/10.1016/S0048-9697(98)00338-6.
[5] J.J.R. Frausto da Silva, R.J.P. Williams, The Biological Chemistry of the Elements, Clarendon Press, Oxford, 2001.
[6] G.E. Camí, M.E. Chacón Villalba, P. Colinas, J. Mol. Struct. 1024 (2012) 110, http://dx.doi.org/10.1016/j.molstruc.2012.05.006.
[7] G. Camí, E. Chacón Villalba, Y. Di Santi, P. Colinas, G. Estiu, D.B. Soria, J. Mol. Struct. 995 (2011) 72, http://dx.doi.org/10.1016/j.molstruc.2011.03.059.
[8] G. Estiu, M.E. Chacón Villalba, G.E. Camí, G.A. Echeverria, D.B. Soria, J. Mol. Struct. 1062 (2014) 82, http://dx.doi.org/10.1016/j.molstruc.2013.11.058.
[9] X.H. Zhao, Y.Y. Zhao, J. Zhang, J.G. Pan, X. Li, Acta Crystallogr., Sect. C 69 (2013) 1332, http://dx.doi.org/10.1107/S010827011302711X.
[10] P.A. Ajibade, G.A. Kolawole, P. O'Brien, M. Helliwell, J. Raftery, Inorg. Chim. Acta 359 (2006) 3111, http://dx.doi.org/10.1016/j.ica.2006.03.030.
[11] J.J. Guo, W. Wang, Y.D. Zhang, L. Yang, S.H. Zhang, Acta Crystallogr., Sect. E: Struct. Rep. Online 68 (2012) m1398, http://dx.doi.org/10.1107/S160053681204336X.
[12] Y.F. Wang, H.L. Zou, X.J. Luo, Z.F. Chen, H. Liang, Acta Crystallogr., Sect. E: Struct. Rep. Online 66 (2010) m548, http://dx.doi.org/10.1107/S1600536810013802.
[13] CrysAlis CCD, CrysAlis RED and associated programs: Oxford Diffraction Program name(s), Oxford Diffraction Ltd, Abingdon, England, 2006.
[14] G.M. Sheldrick, Acta Crystallogr., Sect. A 64 (2008) 112, http://dx.doi.org/10.1107/S0108767307043930.
[15] G.M. Sheldrick, SHELXS-97. Program for Crystal Structure Resolution, Univ. of Göttingen, Göttingen, Germany, 1997.
[16] G.M. Sheldrick, SHELXL-97. Program for Crystal Structures Analysis, Univ. of Göttingen, Göttingen, Germany, 1997.
[17] P. van der Sluis, A.L. Spek, Acta Crystallogr., Sect. A: Found. Crystallogr. 46 (1990) 194, http://dx.doi.org/10.1107/S0108767389011189.
[18] A.L. Spek, PLATON, A Multipurpose Crystallographic Tool, Utrecht University, Utrecht, The Netherlands, 1998.
[19] M. Nardelli, J. Appl. Crystallogr. 32 (1999) 563, http://dx.doi.org/10.1107/S0021889899002666.
[20] L.J. Farrugia, J. Appl. Crystallogr. 32 (1999) 837, http://dx.doi.org/10.1107/S0021889899006020.
[21] W.W. Johnson, M.T. Finley, Handbook of Acute Toxicity of Chemicals to Fish and Aquatic Invertebrates United States Department of the Interior Fish and Wildlife Service, Resource Publication 137, Washington D.C., 1980. p. 1.
[22] F. Bisogno, L. Mascoti, C. Sanchez, F. Garibotto, F. Giannini, M. Kurina-Sanz, R.D. Enriz, J. Agric. Food Chem. 55 (2007) 10635, http://dx.doi.org/10.1021/jf0729098.
[23] M.L. Mascotti, R.D. Enriz, F.A. Giannini, Lat. J. Pharm. 27 (2008) 904.
[24] A.W. Bauer, W.M. Kirby, J.C. Sherris, M. Turk, Am. J. Clin. Pathol. 45 (1966) 493.
[25] F. Rowe, S. Vargas, Diagn. Microbiol. Infect. Dis. 43 (2002) 45, http://dx.doi.org/10.1016/S0732-8893(02)00359-0.
[26] A. Berahou, A. Auhmani, N. Fdil, A. Benharref, M. Jana, C.A. Gadhi, J. Ethnopharmacol. 112 (2007) 426, http://dx.doi.org/10.1016/j.jep.2007.03.032.
[27] T. Mosmann, J. Immunol. Methods 65 (1983) 55.
[28] M. Llunell, D. Casanova, J. Cirera, J. Bofill, P. Alemany, S. Alvarez, et al., SHAPE (2005).
[29] D.M. Adams, A. Dei, A.L. Rheingold, D.N. Hendrickson, J. Am. Chem. Soc. 115 (1993) 8221, http://dx.doi.org/10.1021/ja00071a035.
[30] O.S. Jung, S.H. Park, Y.J. Kim, Y.A. Lee, H.G. Jang, U. Lee, Inorg. Chim. Acta 312 (2001) 93, http://dx.doi.org/10.1016/S0020-1693(00)00346-7.
[31] J. Luo, B.S. Liu, X.G. Zhou, L.H. Weng, Y.R. Li, H.X. Wu, Acta Crystallogr., Sect. C: Cryst. Struct. Commun. 60 (2004) m520, http://dx.doi.org/10.1107/S0108270104020657.
[32] C.A. Hunter, J.K.M. Sanders, J. Am. Chem. Soc. 112 (1990) 5525, http://dx.doi.org/10.1021/ja00170a016.
[33] C.A. Hunter, K.R. Lawson, J. Perkins, J. Chem. Soc., Perkin Trans. 2 (5) (2001) 651.
[34] D.B. Soria, M. Barquín, M.J.G. Garmendia, G. Estiu, J. Coord. Chem. 61 (2008) 3815, http://dx.doi.org/10.1080/00958970802136354.
[35] A.K. Boudalis, C.P. Raptopoulou, A. Terzis, S.P. Perlepes, Polyhedron 23 (2004) 1271, http://dx.doi.org/10.1016/j.poly.2004.02.008.
[36] W.C. Campbell, J. Parasitol. 94 (2008) 934, http://dx.doi.org/10.1645/GE-1413.1.
[37] S. Sharma, N. Anand, Antifolates, in: S. Sharma, N. Anand (Eds.), Approaches to Des. Synth. Antiparasit. Drugs, Pharmacochemistry Library, 1997, p. 439, http://dx.doi.org/10.1016/S0165-7208(97)80040-2.
[38] N.P. Priya, S.V. Arunachalam, N. Sathya, V. Chinnusamy, C. Jayabalakrishnan, Transition Met. Chem. 34 (2009) 437, http://dx.doi.org/10.1007/s11243-009-9214-z.
[39] J. Clover, M. Gowen, Bone 15 (1994) 585, http://dx.doi.org/10.1016/8756-3282(94)90305-0.
[40] C. Fleury, A. Petit, F. Mwale, J. Antoniou, D.J. Zukor, M. Tabrizian, O.L. Huk, Biomaterials 27 (2006) 3351, http://dx.doi.org/10.1016/j.biomaterials.2006.01.035.
[41] M.V. Berridge, P.M. Herst, A.S. Tan, Biotechnol. Annu. Rev. 11 (2005) 127, http://dx.doi.org/10.1016/S1387-2656(05)11004-7.